

Improved conditions for the generation of beta oscillations in the subthalamic nucleus–globus pallidus network

Alex Pavlides,¹ S. John Hogan² and Rafal Bogacz³

¹Bristol Centre for Complexity Sciences, Department of Computer Science, University of Bristol, Bristol BS8 1UB, UK

²Department of Engineering Mathematics, University of Bristol, Bristol, UK

³Department of Computer Science, University of Bristol, Bristol, UK

Keywords: beta oscillations, globus pallidus, Parkinson's disease, subthalamic nucleus

Abstract

A key pathology in the development of Parkinson's disease is the occurrence of persistent beta oscillations, which are correlated with difficulty in movement initiation. We investigated the network model composed of the subthalamic nucleus (STN) and globus pallidus (GP) developed by A. Nevado Holgado *et al.* [(2010) *Journal of Neuroscience*, **30**, 12340–12352], who identified the conditions under which this circuit could generate beta oscillations. Our work extended their analysis by deriving improved analytic stability conditions for realistic values of the synaptic transmission delay between STN and GP neurons. The improved conditions were significantly closer to the results of simulations for the range of synaptic transmission delays measured experimentally. Furthermore, our analysis explained how changes in cortical and striatal input to the STN–GP network influenced oscillations generated by the circuit. As we have identified when a system of mutually connected populations of excitatory and inhibitory neurons can generate oscillations, our results may also find applications in the study of neural oscillations produced by assemblies of excitatory and inhibitory neurons in other brain regions.

Introduction

Parkinson's disease is the second most common neurodegenerative disorder after Alzheimer's disease (Lau & Breteler, 2006). It is estimated that between 4.1 and 4.6 million people in the world's 10 most populous nations are affected. Without intervention this number is set to double to between 8.7 and 9.3 million by 2030 (Dorsey *et al.*, 2007).

The most apparent symptoms of Parkinson's disease include slowness of movement (bradykinesia), tremor and muscle rigidity. These symptoms are accompanied by the death of dopaminergic neurons in the mid-brain substantia nigra pars compacta (Jankovic, 2008), which send strong projections throughout the basal ganglia. The basal ganglia is critically involved in action selection (Redgrave *et al.*, 1999) and damage interrupts its ability to select appropriate actions. In Parkinson's disease, persistent beta oscillations (13–30 Hz) have been observed in the basal ganglia circuits, in particular in the subthalamic nucleus (STN) and globus pallidus (GP) (which is a rat homologue of the GP external in primates) of 6-Hydroxydopamine-lesioned rats (Mallet *et al.*, 2008a,b). Furthermore, the development of persistent beta oscillations is correlated with the severity of one of the symptoms of Parkinson's disease, namely, the patient's inability to successfully initiate movement (Brown, 2003; Chen *et al.*, 2007; Ray *et al.*, 2008).

It is thought that oscillatory activity would be generated in the STN–GP circuit, as experiments *in vivo* have observed beta oscillations in both the STN and GP nuclei, as well as in other basal ganglia

structures (Bevan *et al.*, 2002; Boraud *et al.*, 2005; Mallet *et al.*, 2008a,b). In addition, it was shown by Plenz & Kital (1999) *in vitro* that the STN–GP circuit could produce delta band activity independently. Further evidence supports excitatory–inhibitory architectures being able to produce oscillations (Bevan *et al.*, 2002). However, it has not been shown conclusively that beta oscillations are generated in the STN–GP circuit (Lang & Zadikoff, 2005).

Several computational models have provided insight into actions in the basal ganglia in Parkinson's disease (Gillies *et al.*, 2002; Terman *et al.*, 2002; Rubin & Terman, 2004; Humphries *et al.*, 2006; Leblois *et al.*, 2006; Frank *et al.*, 2007; Kumar *et al.*, 2011). The first model of the basal ganglia showing beta oscillations was by van Albada *et al.* (2009); however, in this model they originate in the cortico-thalamic loops and then spread through the basal ganglia as the disease progresses. The first model of the basal ganglia to show beta oscillations originating in the STN–GP loop was due to Nevado Holgado *et al.* (2010). This model, which included an inhibitory–excitatory connection with time delays between the STN–GP nuclei, was shown to support beta oscillations. Models with time delays display enriched behaviour that would not otherwise occur in models otherwise. In particular, time delays can often be a source of oscillations and instability (Coombes & Laing, 2009). The model reproduced an appreciable amount of physiological data and approximate conditions were derived for the onset of oscillations. Nevertheless, the conditions of stability were quantitatively inaccurate, because an essential parameter determining oscillation onset, the delay time between neural populations, was assumed close to zero. By contrast, experimental data suggest that the synaptic transmission delays between the STN and GP are about 6 ms in rats and monkeys

Correspondence: Alex Pavlides, as above.
E-mail: a.pavlides@bristol.ac.uk

Received 30 November 2011, revised 3 February 2012, accepted 4 March 2012

(Fujimoto & Kita, 1993; Kita *et al.*, 2005). Thus, these delays are not negligible in comparison to other parameters of the population model, e.g. the time constant. [The time constant in a population model is a parameter that describes how rapidly a population of neurons changes its firing rate in response to input. Its value depends mostly on the membrane time constants of individual neurons (Abbott & Dayan, 2001), and has also been proposed to depend on the time constants of synaptic currents (Nevado Holgado *et al.*, 2010).] In this article, we show that there is an alternative approach that extends the validity range of the conditions and, at the same time, is mathematically sounder.

The main derivation of the conditions is provided in the Materials and methods. The Results section is accessible to readers without an extensive mathematical background.

Materials and methods

Description of the model

We begin with a review of the mathematical model described by Nevado Holgado *et al.* (2010), which investigated the STN–GP circuit shown in Fig. 1A. Here the STN neural population projects excitatory glutamatergic axons to the GP, and the GP neural population projects inhibitory GABAergic axons back to the STN as well as to other

neurons within the GP. The GP receives inhibitory input from the striatum and the STN receives excitatory input from the cortex.

Using the equation for the mean firing-rate model described in Abbott & Dayan (2001) and Vogels *et al.* (2005), the corresponding equations describing this system are

$$\tau_S S'(t) = F_S(-w_{GS}G(t - T_{GS}) + w_{CS}Ctx) - S(t) \quad (1)$$

$$\tau_G G'(t) = F_G(w_{SG}S(t - T_{SG}) - w_{GG}G(t - T_{GG}) - w_{XG}Str) - G(t) \quad (2)$$

where $S(t)$ and $G(t)$ are the firing rates of the STN and GP respectively, $G(t - T_{GS})$, $S(t - T_{SG})$ and $G(t - T_{GG})$ are the delayed firing rates, τ_S and τ_G are the time constants of the STN and GP populations (see above) and w represents the various weights between neural populations. The subscripts indicate the population from which the signal originates and where the signal is received. For instance, w_{GS} describes the strength of connection from the GP population to the STN population, w_{SG} gives the strength between the STN and GP populations and w_{GG} is the strength of the self-inhibitory connection of the GP population. The weights w_{CS} and w_{XG} are the strength of input connection from the cortex to STN and the striatum to GP, respectively. F_S and F_G are the activation functions of the STN and GP neural populations, which describe their firing rate as a function of synaptic input.

The sigmoid activation functions $F_S(in)$ and $F_G(in)$, given by Eqns 3 and 4, have been shown to approximate a population of neurons with heterogeneous activation functions (Wilson & Cowan, 1972).

$$F_S(in) = \frac{M_S}{1 + \left(\frac{M_S - B_S}{B_S}\right) \exp(-4in/M_S)} \quad (3)$$

$$F_G(in) = \frac{M_G}{1 + \left(\frac{M_G - B_G}{B_G}\right) \exp(-4in/M_G)} \quad (4)$$

The constants M_S and M_G are the maximum firing rates of each population, and B_S and B_G are the population firing rates in the absence of input. The other two parameters needed to define a sigmoid curve are the minimum firing rate, which is set to zero (as often seen in experiments), and the slope, which is set to 1 for a simple interpretation of synaptic weight units (Nevado Holgado *et al.*, 2010). These curves are shown in Fig. 1B.

The parameters summarized in Table 1 were available in the literature (for details, see Nevado Holgado *et al.*, 2010). However, the synaptic weights were not available in the literature and therefore Nevado Holgado *et al.* (2010) found the values for which the model reproduced a wide range of experimental findings. The values of those

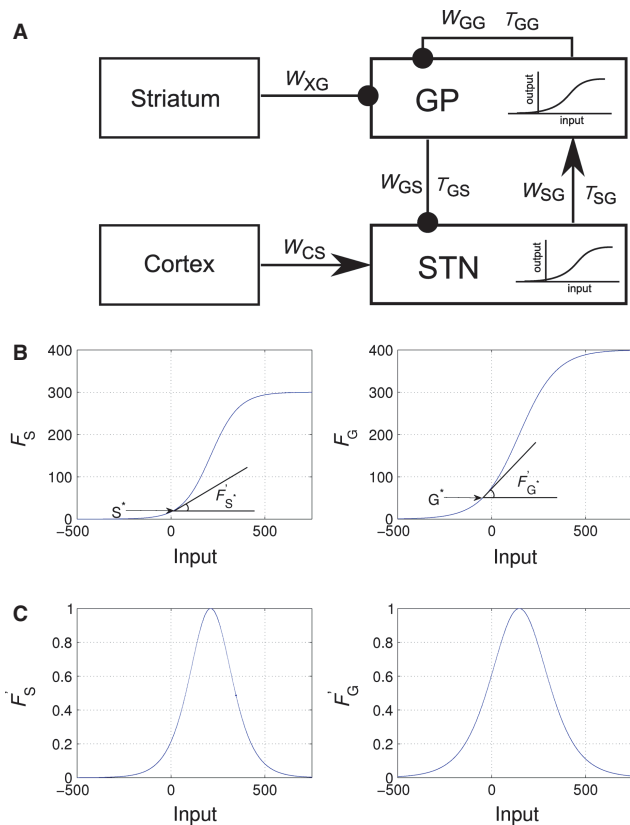


FIG. 1. (A) Schematic of the STN–GP model considered in this article. Each rectangle denotes a neural population, arrows denote excitatory signals and lines ending in circles represent inhibitory signals. Alongside these are the symbols used to represent weights w and time delays T for each connection. (B) Output from the activation functions, $F_S(in)$ and $F_G(in)$, given by Eqns 3 and 4. Drawn tangent to the activation function curves are their derivatives at the fixed points, F'_{S^*} and F'_{G^*} , corresponding in this case to the simulations shown in Fig. 2. (C) Derivatives of the activation function from Panel B.

TABLE 1. The parameters and their values used in the model along with the sources for this information

Parameter	Value	Source
T	6 ms	Fujimoto & Kita (1993), Kita <i>et al.</i> (2005)
τ_S	6 ms	Kita <i>et al.</i> (1983), Nakanishi <i>et al.</i> (1987), Paz <i>et al.</i> (2005)
τ_G	14 ms	Kita & Kitai (1991)
Ctx	27 spk/s	Lebedev & Wise (2000)
Str	2 spk/s	Schultz & Romo (1988)
M_S	300 spk/s	Hallworth <i>et al.</i> (2003)
B_S	17 spk/s	Hallworth <i>et al.</i> (2003)
M_G	400 spk/s	Kita <i>et al.</i> (2005), Kita (2007)
B_G	75 spk/s	Kita <i>et al.</i> (2004), Kita (2007)

parameters for both the healthy and Parkinsonian state are summarized in Table 2.

We show the behaviour of the model, corresponding to Eqns 1–4, for the values of weights corresponding to the healthy and Parkinsonian state in Fig. 2. Please note that, for the parameters corresponding to the healthy state, the system converges to a constant firing rate (i.e. a fixed point of the system), whereas for the parameter corresponding to the Parkinsonian state it produces sustained oscillations.

TABLE 2. The model parameter values for synaptic connection weights estimated by Nevado Holgado *et al.* (2010) for both healthy and Parkinson's disease states

Parameter	Healthy state	Parkinson's disease
w_{GS}	1.12	10.7
w_{SG}	19.0	20.0
w_{GG}	6.60	12.3
w_{CS}	2.42	9.2
w_{XG}	15.1	139.4

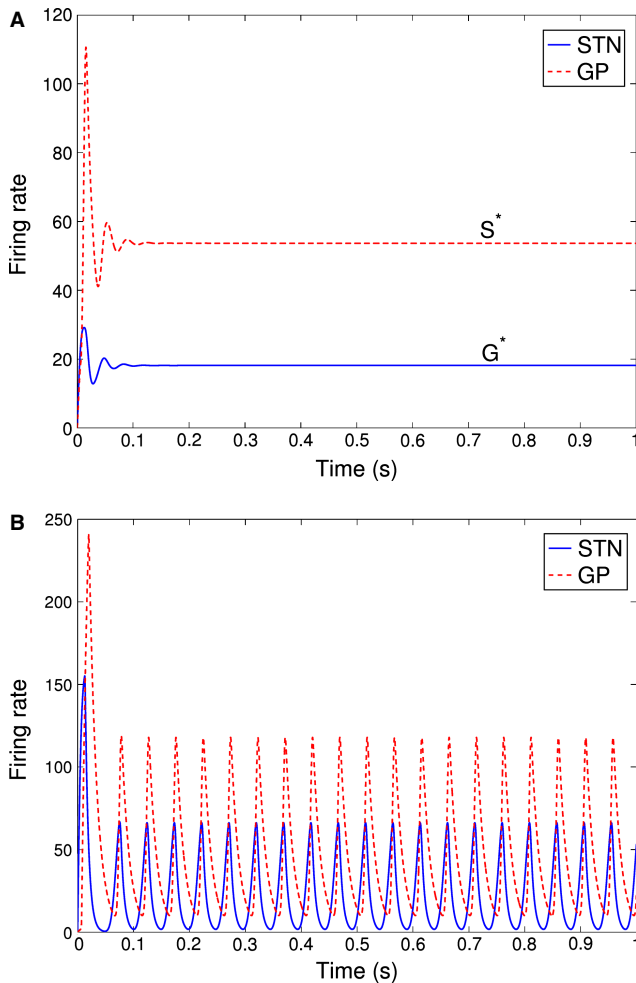


FIG. 2. Numerical simulation of the nonlinear system, which shows the bifurcation that occurs in firing rate between the healthy-type behaviour (A) and the Parkinsonian-type behaviour (B). Estimated weight parameters for both the healthy state and Parkinsonian state were obtained from Nevado Holgado *et al.* (2010) (Table 2). The system tends towards the stable fixed points, S^* and G^* , in healthy behaviour, and the system orbits around these fixed points producing oscillations in Parkinsonian behaviour.

Original stability analysis

This section will review the stability conditions as described in Nevado Holgado *et al.* (2010) before providing details of our new analysis. The authors made the following simplifying assumptions: (i) the membrane time constants τ_S and τ_G were taken to have an average value of $\tau = 10$ ms; (ii) the transmission delays for the separate neural populations T_{SG} , T_{GS} and T_{GG} were taken to be equal, denoted by the single variable T ; and (iii) the nonlinear activation functions were replaced with linear functions. We shall refer to this simplified system as the linear system described by Eqns 5 and 6.

$$\tau S'(t) = -w_{GS}G(t-T) + w_{CS}Ctx - S(t) \quad (5)$$

$$\tau G'(t) = w_{SG}S(t-T) - w_{GG}G(t-T) - w_{XG}Str - G(t) \quad (6)$$

We could solve these equations by replacing the time delayed variables with a Taylor series expansion around zero, leading to Eqns 7 and 8. This simplification works well for small values of the time delay. However, in general, it is not recommended (Mazanov & Tognetti, 1974) because it is inaccurate for large delay values.

$$\tau S'(t) = w_{GS}(G(t) - \Delta t \cdot G'(t)) + w_{CS}Ctx - S(t) \quad (7)$$

$$\tau G'(t) = w_{SG}(S(t) - \Delta t \cdot S'(t)) - w_{GG}(G(t) - \Delta t \cdot G'(t)) + w_{XG}Str - G(t) \quad (8)$$

Using parameters representing Parkinson's disease, the linear Eqns 7 and 8 produce divergent oscillations, whereas in the nonlinear model the nondiverging oscillations correspond to a stable limit cycle. This divergence can be remedied by imposing the realistic boundary condition that firing rates cannot be negative (Nevado Holgado *et al.*, 2010). For oscillations to occur in the linear system, the fixed point must be unstable and trajectories starting from its neighbourhood must form spirals as opposed to a limit cycle. A boundary restricts the spiral trajectory, thereby producing oscillations of constant amplitude. These behaviours occur when Eqns 9 and 10 are satisfied. The third condition, Eqn 11, is required to form a closed loop trajectory in the phase plane.

$$w_{GS}w_{SG}\frac{T}{\tau} > 1 + w_{GG}(1 - \frac{T}{\tau})/2 \quad (9)$$

$$w_{SG}w_{GS} > \frac{w_{GG}^2}{4} \quad (10)$$

$$w_{SG}w_{CS}Ctx > w_{XG}Str \quad (11)$$

New stability analysis

In this section, we find the stability of the system described by Eqns 5 and 6 for the case of arbitrary values of the delay, in the absence of cortical or striatal input (as they do not change the stability conditions for the linear system). Eqns 5 and 6 can be rewritten as Eqn 12, where the matrices A and B are given by Eqns 13 and 14.

$$\begin{bmatrix} S'(t) \\ G'(t) \end{bmatrix} + A \begin{bmatrix} S(t-T) \\ G(t-T) \end{bmatrix} + B \begin{bmatrix} S(t) \\ G(t) \end{bmatrix} = 0 \quad (12)$$

$$A = \begin{bmatrix} 0 & \frac{w_{GS}}{\tau} \\ -\frac{w_{SG}}{\tau} & \frac{w_{GG}}{\tau} \end{bmatrix} \quad (13)$$

$$B = \begin{bmatrix} \frac{1}{\tau} & 0 \\ 0 & \frac{1}{\tau} \end{bmatrix} \tag{14}$$

We solve Eqns 12–14 using Laplace transforms. This is equivalent to mapping our equations from the time domain into the frequency domain where the inputs and outputs become functions of complex angular frequency. A useful property of the Laplace transform is that the Laplace transform of $f(t - T)$ is given by $F(s)$ multiplied by a phase term e^{-Ts} . This is known as the First Shifting Theorem and is given by Eqn 15 for any arbitrary constant, $T > 0$.

$$L\{f(t - T)\} = e^{-Ts}F(s) \tag{15}$$

Taking the Laplace transform of Eqn 12 and using this result we get

$$-\begin{bmatrix} S(0) \\ G(0) \end{bmatrix} + s \begin{bmatrix} S(s) \\ G(s) \end{bmatrix} + Ae^{-sT} \begin{bmatrix} S(s) \\ G(s) \end{bmatrix} + B \begin{bmatrix} S(s) \\ G(s) \end{bmatrix} = 0 \tag{16}$$

Without loss of generality, we set $\begin{bmatrix} S(0) \\ G(0) \end{bmatrix} = 0$ and so

$$sI + Ae^{-sT} + B = 0 \tag{17}$$

Taking the determinant of both sides, we get the (transcendental) characteristic equation for the eigenvalues s , given by

$$\det(sI + Ae^{-sT} + B) = 0 \tag{18}$$

In the analysis of ordinary differential equations without delays, we must find the location of a finite number of eigenvalues to determine the stability boundaries of the system. If $T = 0$, then s , which satisfies Eqn 18, would be the eigenvalues of the matrix $A + B$, and the sign of the real part of s would determine the stability. Analogously here, any s satisfying Eqn 18 is an eigenvalue of the delayed system. Delay differential equations have an infinite number of eigenvalues, introduced by the e^{-sT} term. Therefore, the stability boundary of the system is more easily determined by finding when the real part of the eigenvalues changes from negative to positive, indicating the change from stable to unstable. For this reason we substitute $s = i\lambda$ into Eqn 18 and expand the exponential to give

$$\begin{aligned} &-\lambda^2 + i\lambda w_{GG} \cos(\lambda T) + \lambda w_{GG} \sin(\lambda T) + \frac{2i\lambda}{\tau} + w_{GG} \cos(\lambda T) \\ &- w_{GG}i \sin(\lambda T) + \frac{1}{\tau^2} + w_{SG}w_{GS} \cos(2\lambda T) - iw_{SG}w_{GS} \sin(2\lambda T) = 0 \end{aligned} \tag{19}$$

Linear model without intrinsic globus pallidus connectivity

We first derive conditions for oscillations valid for arbitrary delay values when there is no intrinsic GP connectivity. Therefore, we set $w_{GG} = 0$ in Eqn 19. We also set the membrane time constant $\tau = 1$, which can be interpreted as a rescaling of time $\hat{T} = \frac{T}{\tau}$. By taking real and imaginary parts, we find

$$0 = 1 - \lambda^2 + w_{SG}w_{GS} \cos(2\lambda\hat{T}) \tag{20}$$

$$0 = 2\lambda - w_{SG}w_{GS} \sin(2\lambda\hat{T}) \tag{21}$$

By squaring and adding Eqns 20 and 21, we obtain a quartic equation in λ . Two of the roots give λ imaginary, contrary to our assumption. Hence we find

$$\lambda = \sqrt{w_{GS}w_{SG} - 1} \tag{22}$$

We then substitute Eqn 22 back into Eqn 20 to give a final expression linking the parameters we are interested in $2-w_{GS}w_{SG}+w_{SG}w_{GS}\cos(2\lambda\hat{T})=0$.

Finally, we can write an exact expression for the delay time \hat{T} for any value of the product of the connection weights, $w_{GS}w_{SG}$

$$\hat{T} = \frac{1}{2\sqrt{w_{GS}w_{SG}-1}} \arccos\left(1 - \frac{2}{w_{GS}w_{SG}}\right) \tag{24}$$

Linear model including intrinsic globus pallidus connectivity

We have shown that oscillatory behaviour can be generated with the exclusion of w_{GG} . However, it is more biologically realistic to include it in our model of the basal ganglia. For this reason, the general solution to Eqn 18 was sought, which would hold for larger time delays. An analytic approach similar to the case $w_{GG} = 0$ led to cumbersome expressions. A more elegant and straightforward approach to the general solution has been developed by Asl & Ulsoy (2003) in connection with chattering problems in engineering. We will show that this method can be applied to solve the general case of $w_{GG} \neq 0$. For this method to work, our matrices A and B must commute. However, as B is diagonal, this condition is satisfied. We can rewrite the characteristic Eqn 17 as

$$sIe^{\hat{s}\hat{T}} + Be^{\hat{s}\hat{T}} = -A \tag{25}$$

As it is possible to show that

$$Ie^{\hat{s}\hat{T}} = e^{Is\hat{T}} \tag{26}$$

we can now rewrite Eqn 25 as

$$(sI + B)\hat{T}e^{(sI+B)\hat{T}} = -A\hat{T}e^{B\hat{T}} \tag{27}$$

Now, the Lambert W function is given by

$$W(x)e^{W(x)} = x \tag{28}$$

Therefore, if we have an equation of the form $y = xe^x$ it can be rewritten as $x = W(y)$. Eqn 27 becomes

$$(sI + B)\hat{T} = W(-A\hat{T}e^{B\hat{T}}) \tag{29}$$

Rewriting Eqn 29 leads to an expression for the eigenvalues of the characteristic Eqn 17

$$sI = \frac{1}{\hat{T}} W(-A\hat{T}e^{B\hat{T}}) - B \tag{30}$$

Therefore, the stability boundary of the system can be calculated from

$$\det\left[sI - \frac{1}{\hat{T}} W(-A\hat{T}e^{B\hat{T}}) + B\right] = 0 \tag{31}$$

To locate the stability boundary we find s , which satisfies Eqn 31 for a given set of parameters. If the real part of s satisfies, $Re(s) < 0$, the system is stable.

Inclusion of sigmoid activation function

The inclusion of the sigmoid activation function complicates the situation. However, we can make analytic progress by linearizing the function and then following the same procedures outlined previously. The result is the characteristic equation

$$sI + \tilde{A}e^{-s\hat{T}} + B = 0 \tag{32}$$

where

$$\tilde{A} = \begin{bmatrix} 0 & \frac{F'_{S^*} w_{GS}}{\tau} \\ \frac{-F'_{G^*} w_{SG}}{\tau} & \frac{F'_{G^*} w_{GG}}{\tau} \end{bmatrix} \tag{33}$$

The derivatives of the activation functions in Eqn 33 can be written as

$$F'_{S^*} = F'_S(-w_{GS}G^*(t) + w_{CS}Ctx) \tag{34}$$

$$F'_{G^*} = F'_G(w_{SG}S^*(t) + w_{GG}G^*(t) - w_{XG}Str) \tag{35}$$

If we solve Eqn 32 we find that the stability boundary has been shifted by the derivatives of the sigmoid functions at the fixed point of the system. The stability boundary when $w_{GG} = 0$ is

$$\hat{T} = \frac{1}{2\sqrt{w_{SG}F'_{S^*}w_{GS}F'_{G^*}} - 1} \arccos\left(1 - \frac{2}{w_{SG}F'_{S^*}w_{GS}F'_{G^*}}\right) \tag{36}$$

When we include intrinsic GP connectivity we get

$$\det\left[sI - \frac{1}{\hat{T}}W(-\tilde{A}\hat{T}e^{s\hat{T}}) + B\right] = 0 \tag{37}$$

where matrix \tilde{A} is given by Eqn 33.

Details of simulations

We solved Eqns 1 and 2 using DDE23 in MATLAB, which is well documented (Shampine & Thompson, 2001).

To find the stability boundary of the nonlinear model, we first required the fixed points of the system, given by S^* and G^* . This was achieved by minimizing Eqn 38 for different values of w_{SG} and w_{GS}

$$K = -[S(t) + F_S(-w_{GS}G(t) + w_{CS}Ctx)]^2 + [-G(t) + F_G(w_{SG}S(t) - w_{GG}G(t) - w_{XG}Str)]^2 \tag{38}$$

For each pair of w_{SG} and w_{GS} we calculate S^* and G^* . These values could then be substituted into Eqns 34 and 35 to give F'_{S^*} and F'_{G^*} . Using these we could calculate the stability boundary from Eqns 36 and 37 for different values of the time delay. Eqn 37 is stable when the real part of the eigenvalues satisfies, $Re(s) \leq 0$, for a given set of parameters.

The criterion for oscillation onset, in numerical simulations, is the set of parameters that correspond to a sustained increase in oscillation amplitude. When we investigate the effect of cortical and striatal inputs on the stability boundary, the criterion for oscillation onset is that there are sustained oscillations with amplitude between 4 and 7 spk/s. In all numerical simulations, oscillations at the stability

boundary have small amplitudes that increase as we raise the parameter values and move further from the boundaries.

It should also be noted that the value of the connectivity among GP neurons $w_{GG} = 1$ was chosen for simplicity and because there was numeric instability when $w_{GG} = 6.6$ when using Eqns 31 and 37. However, we have shown that the effect of $w_{GG} = 1$ is to increase the value of $w_{SG}w_{GS}$ needed for oscillation onset to occur when compared with $w_{GG} = 0$.

Results

In the previous section we derived conditions for oscillation onset, for the model of the STN–GP network, shown schematically in Fig. 1A. Importantly, these conditions were obtained without the assumption that the synaptic transmission was close to zero, in contrast to the previously derived stability conditions of Nevado Holgado *et al.* (2010), who made this assumption. In this section we compare these two sets of conditions with numerical simulations of the models.

The Results section is split into two parts reflecting the work in the Materials and methods. The first part deals with a linear model that makes the simplifying assumption that the firing rate of the neural populations changes linearly with their inputs. The second part deals with the nonlinear model that makes the more realistic assumption that the firing rate of the neural populations varies as a sigmoidal function of their inputs (Wilson & Cowan, 1972) (see Fig. 1B). We consider here two cases of each of these models. (i) A simplified model not including the self-interaction of GP neurons, we set $w_{GG} = 0$. We consider this case for two reasons. Firstly, in the article by Nevado Holgado *et al.* (2010), it was shown that intrinsic GP connectivity was not essential for beta wave generation. Secondly, as we will show, an analytic solution is possible and this provides useful insight into the case when intrinsic GP connectivity is present. (ii) The inclusion of the GP self-interaction by setting $w_{GG} \neq 0$. In this way we progress towards the most general result, gaining insight into the system as we progress.

Linear model without intrinsic globus pallidus connectivity

Eqn 39 is the condition that the parameters of the model need to satisfy in order for the system to generate oscillations and Eqn 40 is the approximate condition derived by Nevado Holgado *et al.* (2010).

$$\frac{T}{\tau} > \frac{1}{2\sqrt{w_{GS}w_{SG}} - 1} \arccos\left(1 - \frac{2}{w_{GS}w_{SG}}\right) \tag{39}$$

$$\frac{T}{\tau} > w_{GS}w_{SG} \tag{40}$$

In the inequalities, w_{GS} and w_{SG} denote the strengths of synaptic connections between the neural populations shown in Fig. 1A, T is the synaptic transmission delay and τ is the membrane time constant of the neurons. Both conditions predict that, for oscillations to occur, the weights of the connections between the STN and GP, as well as the synaptic transmission delay, must be sufficiently high with respect to the membrane time constant. Furthermore, in the limit that $T \rightarrow 0$, both conditions require that $w_{GS}w_{SG} \rightarrow \infty$.

Figure 3A shows that the condition given by Eqn 39 matches better when oscillations occur in simulations than Eqn 40. This is particularly true when T is much larger than zero.

According to Nevado Holgado *et al.* (2010), the biologically relevant region, once scaling is taken into account, corresponds to the range $T/\tau = 0.6\text{--}0.8$ s of the time delay. In this region we can see a significant improvement, approximately 30%, in the position of the stability boundary.

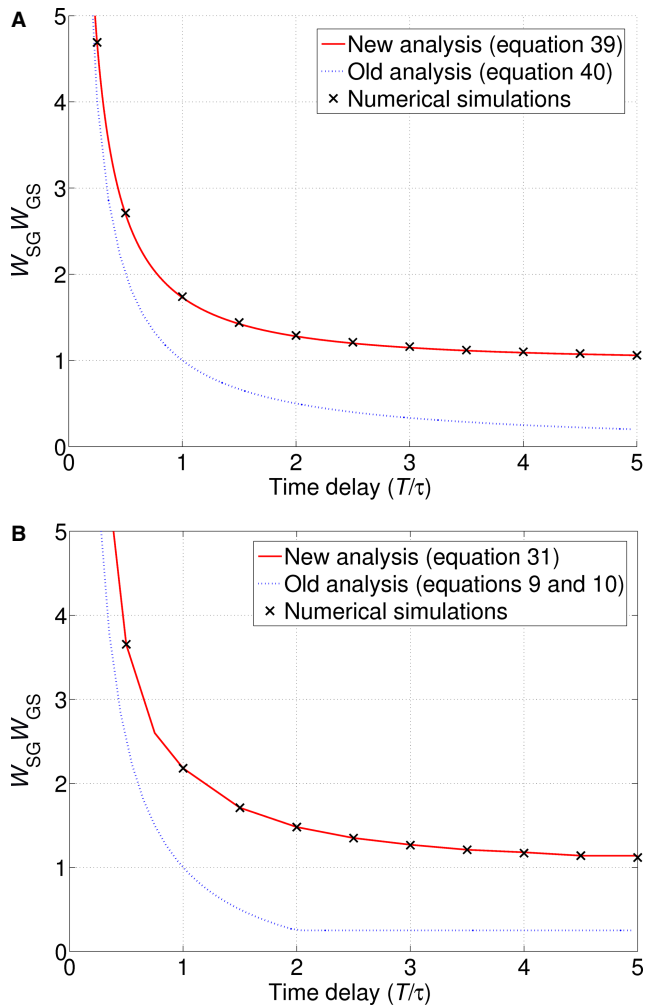


FIG. 3. Comparisons of the conditions for oscillation onset, for the linear models, with numerical simulations. The STN–GP circuit is unstable, and therefore oscillatory, when its parameters correspond to the region above the curves. Conversely the system is stable when it is below the curves. (A) The stability boundary for the linear system without intrinsic GP connectivity ($w_{GG} = 0$). Simulations show that the onset of oscillations occurs very close to the stability boundary calculated from Eqn 39 even for long time delays. This is in contrast to the previous conditions, Eqn 40, which compares less well at larger delay values. (B) Linear system including intrinsic GP connectivity ($w_{GG} = 1$). The stability boundary approximation from Eqn 31 compares well with simulation and is significantly better than the earlier approximation given by Eqn 41, from Nevado Holgado *et al.* (2010).

For long time delays, which may be relevant for other systems, the conditions differ significantly in their predictions. The inequality (40) of Nevado Holgado *et al.* (2010) implies that as $T \rightarrow \infty$, the weights $w_{SG} w_{GS}$ can be just slightly above zero for the model to oscillate. By contrast, the right-hand side of inequality (39) is only defined for $w_{SG} w_{GS} > 1$, implying that, no matter how long the delay is, $w_{SG} w_{GS}$ has to be higher than 1 for the system to oscillate, as also seen in the simulation of Fig. 3A. In the limit that $T \rightarrow \infty$, the lowest $w_{SG} w_{GS}$ for which (39) is satisfied converges to 1.

Linear model including intrinsic globus pallidus connectivity

When we include connections among GP neurons it is no longer possible to derive an inequality for the parameters that the model must satisfy to produce oscillations. Therefore, in the Materials and methods we

showed that the stability boundary of the linear model with intrinsic GP connectivity can be found by numerically solving Eqn 31. Figure 3B compares Eqn 31 and the combined conditions 9 and 10 (Nevado Holgado *et al.*, 2010) with numerical simulation. We see a significant improvement in the approximation of the stability boundary.

Nonlinear model

The inclusion of the nonlinear sigmoid makes the results more complicated but does provide useful insights. We have shown how to derive the stability boundary from the linearized equations in the Methods and materials. To summarize, the expression for the case without intrinsic GP connectivity is given by Eqn 41. The stability boundary includes the derivatives of the sigmoid functions at the fixed points of the system, for which we will now provide intuition. A fixed point is defined as the activity levels of the STN and GP at which the activity does not change. For example, in the numerical simulation of Fig. 2A, the activity levels of the STN and GP converge to stable values, which we denote by S^* and G^* . If the system oscillates (Fig. 2B), the activity levels oscillate around the fixed point. The values of the fixed points from Fig. 2A are also indicated in Fig. 1B. Terms F'_{S^*} and F'_{G^*} are defined as slopes of lines tangent to the sigmoid functions at the fixed points (see Fig. 1B and C). F'_{S^*} and F'_{G^*} describe how much the neural populations change their activity level due to synaptic input. For example, according to Fig. 1B, if STN activity is very close to zero, then small changes in the input have no effect on the activity (this corresponds to a situation when all neurons are highly hyperpolarized). By contrast, when STN activity is around 150 Hz, the STN neurons react strongly to their input. In inequality 41, the slopes of the sigmoid functions multiply the weights between the STN and GP. This expresses the fact that, for the system to oscillate, not only must the synaptic connections between the STN and GP be sufficiently high but the STN and GP firing rates must be such that the neural populations react to their inputs. In the next section we will discuss how F'_{S^*} and F'_{G^*} are modified by cortical and striatal inputs. As the product of these derivatives is always ≤ 1 , the product of $w_{SG} w_{GS}$ is always larger than the corresponding linear case for a given T/τ .

$$\frac{T}{\tau} > \frac{1}{2\sqrt{w_{SG} F'_{S^*} w_{GS} F'_{G^*} - 1}} \arccos\left(1 - \frac{2}{w_{SG} F'_{S^*} w_{GS} F'_{G^*}}\right) \quad (41)$$

Evaluating inequality 41 for different values of delay agrees very well with the simulations shown in Fig. 4A.

If we include the intrinsic GP connectivity, its effect is to slightly increase the values of $w_{SG} w_{GS}$ at which oscillations occur (Fig. 4B) in comparison to the case when $w_{GG} = 0$. This is due to w_{GG} introducing decay into the activity levels of the GP. An increase in the product $w_{SG} w_{GS}$ is therefore required to balance out the influence of w_{GG} and allow oscillations between the STN and GP populations.

Effect of cortical and striatal inputs on the model

A feature of the nonlinear model is that it introduces the activity levels of the cortex and striatum in the condition for oscillation through the terms F'_{S^*} and F'_{G^*} , which were not included in the linear models.

We used the linearized model without intrinsic GP connectivity $w_{GG} = 0$ and the unhealthy weights of Table 2. For the case when $w_{GG} \neq 0$, the intrinsic connectivity does not significantly alter the influence that the cortical and striatal inputs have on the system. For this reason we chose to focus on the case $w_{GG} = 0$, which is more straightforward yet displays similar behaviour.

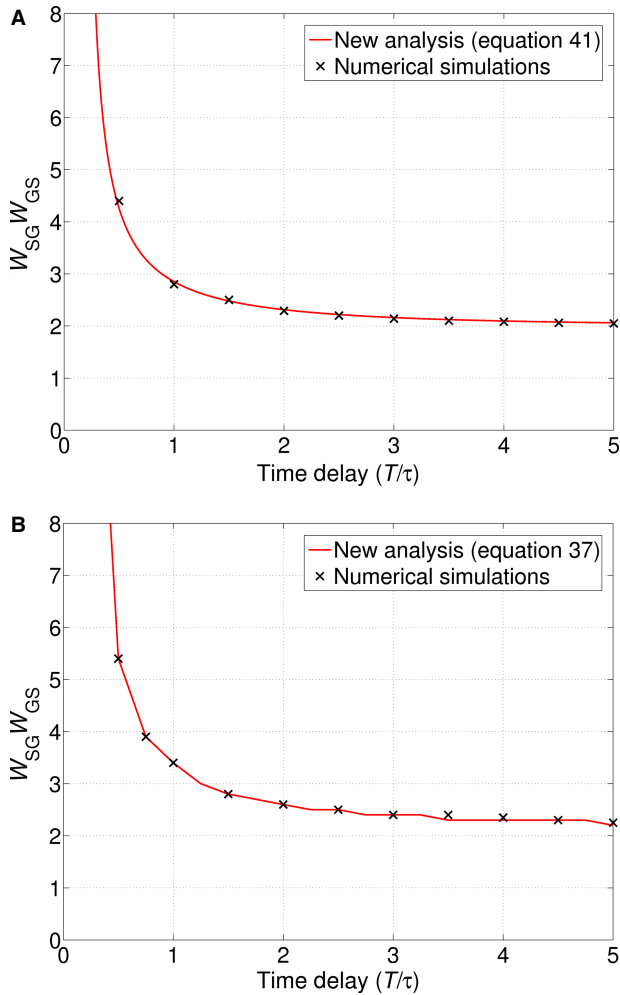


FIG. 4. Comparisons of the conditions for oscillation onset, for the nonlinear models, with numerical simulations. The STN–GP circuit is unstable, and therefore oscillatory, when the parameters correspond to the region above the curves. Conversely the system is stable when it is below the curves. (A) The stability boundary for the nonlinear system without intrinsic GP connectivity ($w_{GG} = 0$). The numerical solution compares very well with simulation of the nonlinear model for all values of the time delay. (B) The region of stability for the nonlinear system with intrinsic GP connectivity ($w_{GG} = 1$). At the stability boundary the numerical solution compares very well with simulation of the nonlinear model for all values of the time delay. In both cases, cortical and striatal inputs are also included with values: $w_{CS} = 9.2$, $w_{XG} = 139.4$, $Ctx = 27$, $Str = 2$.

Figure 5 shows for what values of the cortical and striatal inputs the model produces oscillations and below we provide intuition of why it happens. On the basis of Fig. 1A we can infer that, as we increase cortical input, both fixed points, S^* and G^* , will increase. This happens because cortical input has an excitatory effect directly on the STN and indirectly on the GP. This leads to an initial increase in F'_{S^*} and F'_{G^*} and then a subsequent decrease, as the cortical input continues to rise, as shown in Fig. 1C. However, it is important to note that, generally, the STN and GP are unlikely to produce sustained activity above 200 Hz. The system is therefore unlikely to reach a point where the value of F'_{S^*} and F'_{G^*} begins to diminish because of ever-rising inputs. In particular, we would not see very high cortical inputs where the activation functions become saturated, effectively decoupling the neural populations from each other.

The effect of striatal input is a bit more complicated. Figure 5 shows that, if we start in a nonoscillatory region and increase the

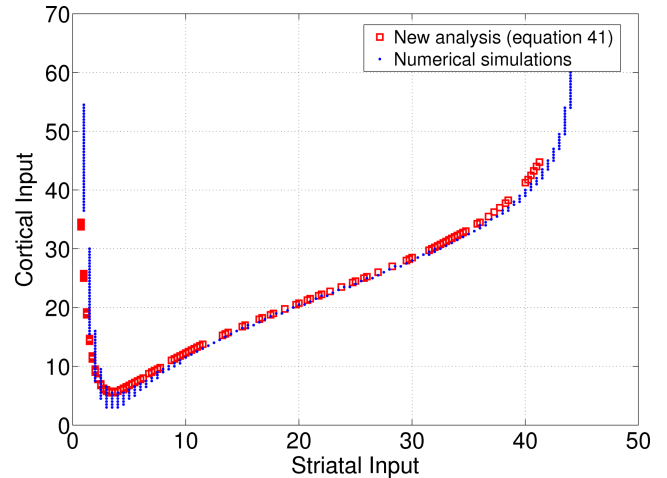


FIG. 5. The effect of striatal and cortical input on the stability boundary for parameters associated with Parkinson’s disease and $w_{GG} = 0$. The system is oscillatory when its inputs correspond to the region above the curves and it is stable when below the curves. It can be seen that oscillation onset can be initiated by an increase in either cortical or striatal input. For fixed cortical input, an increase in striatal input will push the system from a stable region (point A), to an unstable oscillatory region (point B), and back to a stable region again (point C).

striatal input, we can push the system into an oscillatory region. As the striatal input is increased further, the oscillations will stop. In terms of the fixed points, if there is an increase in the striatal input we will see an increase in S^* but a decrease in G^* . This is because the striatum has an inhibitory influence on the GP (Fig. 1A) and therefore the inhibitory influence of the GP on the STN is lessened, leading to an increase in the STN firing rate.

The reason for this behaviour can be understood by reference to Fig. 6 and Eqn 41, which will allow us to investigate how the left-hand side of the inequality changes as we increase the striatal input and therefore change the fixed points of the system. Figure 6A–C shows the outputs of the STN and GP populations for three different striatal inputs, indicated by points A, B and C in Fig. 5. Figure 6A shows the fixed points of the system corresponding to a healthy individual. Note that the STN is quite subdued because, although it receives input from the cortex, it receives a large inhibitory input from the GP. The system can be said to be generally inhibited, F'_{S^*} is small, and therefore inequality 41 is not satisfied and oscillations do not occur. In Fig. 6B an increase in the striatal input inhibits the GP population, which in turn reduces its inhibitory influence over the STN. The STN is therefore more excitatory and its output is increased (Fig. 6B). In terms of Eqn 41, what has occurred is that, although F'_{G^*} has been slightly reduced, F'_{S^*} has been substantially increased so that the product of the activation function derivatives F'_{S^*} and F'_{G^*} has been increased causing oscillation onset. In Fig. 6C, as the striatal input continues to increase, we return to a situation, as in Fig. 6A, in which the product of F'_{S^*} and F'_{G^*} is again low and therefore oscillation does not occur.

Discussion

We have confirmed previous work by Nevado Holgado *et al.* (2010) showing which parameters were important for the onset of oscillations in the basal ganglia. The frequency of these oscillations is influenced mainly by two factors, discussed in depth by Nevado Holgado *et al.* (2010), which are the time delay T and the membrane time constant τ ,

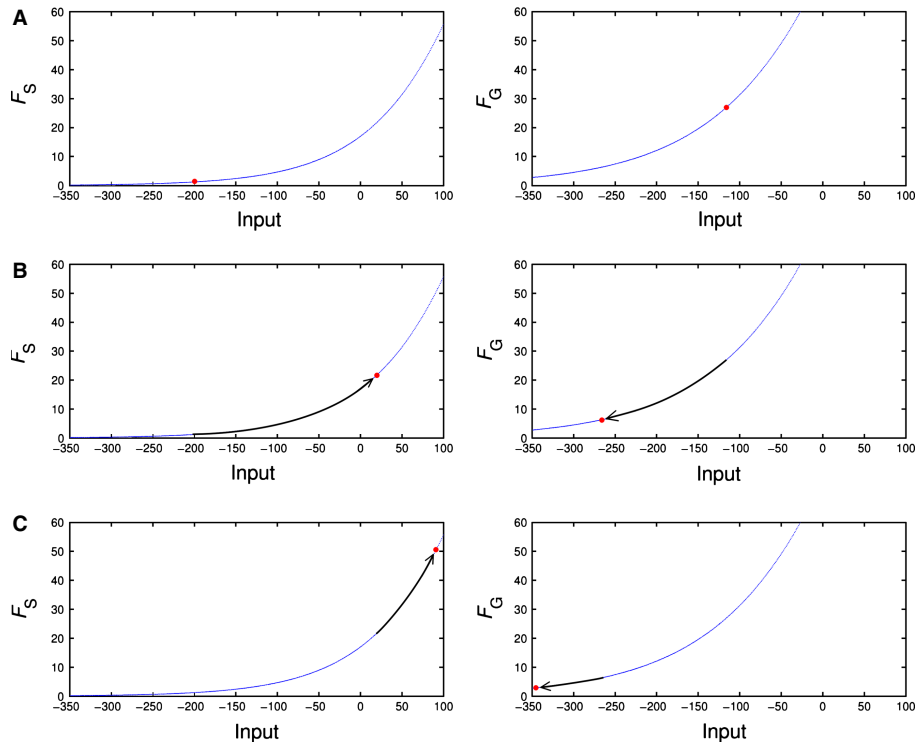


FIG. 6. The points in A, B and C correspond to the fixed points of the system at the marked points A, B and C in Fig. 5. It illustrates how the outputs of the activation functions are changed by an increase in the striatal input. In A we see healthy-type behaviour where the GP population is effectively inhibiting the STN population. In B we see that, although F_{G^*} has been slightly reduced, F_{S^*} has been substantially increased so that the product of the activation function derivatives F'_{S^*} and F'_{G^*} has been increased causing oscillation onset. In C we see that, when striatal input is very large, it significantly suppresses the firing rate of the GP population and oscillations stop.

which determine how long it takes for information to traverse the STN–GP loop.

Using experimentally measured parameters (Table 2), it was shown how this model could produce beta oscillations in the range 13–20 Hz. However, whereas the earlier work was qualitatively accurate, we have quantitatively improved on the conditions in both the linear and nonlinear models. In particular, the previous work suggested that, as the time delay increased, the strength of synaptic connections between STN and GP neurons required for oscillations tended to zero, which is inconsistent with the results of simulations. In contrast, our results are valid for arbitrary large time delays. In the biologically relevant region, $T/\tau = 0.6$ – 0.8 s, with $w_{GG} = 1$ the difference between $w_{SG}w_{GS}$ required for oscillations suggested by the two methods was approximately 30–50%. As explained in the Introduction, the time delay is an important parameter that enriches the behaviour of our system and is essential for oscillation generation in this circuit. In particular, it is seen here that, as the synaptic delay time T increases, a lower value of the connection weights $w_{SG}w_{GS}$ is required for oscillation onset.

Relationship to previous modelling studies

The relationship of the model with previous works (Gillies *et al.*, 2002; Terman *et al.*, 2002; Humphries *et al.*, 2006; Leblois *et al.*, 2006) was discussed by Nevado Holgado *et al.* (2010); however, for completeness we will give a brief overview. The model by Gillies *et al.* (2002) used a mean firing-rate model of the STN–GP network that was simple enough to enable mathematical analysis and provide conditions for oscillation onset. In this study, all parameters were

obtained from experiments except for the network weights. They then showed that there existed three states corresponding to stable, bistable and oscillatory behaviour for different values of the connection weights. It differed from the model analysed here in that it omitted synaptic transmission delay between neural populations. In addition, it assumed the existence of connections among STN neurons, which was crucial for oscillation onset in the model. However, experimental evidence for these connections is not sufficiently strong so they are not included in our model. The model by Leblois *et al.* (2006) provided a detailed account of action selection in the basal ganglia. Using a reduced model to gain further insights, they showed that synchronous oscillations did occur for reduced dopamine levels but that the frequency of these oscillations was ~ 10 – 12 Hz, which was outside the beta band range. The remaining articles in the literature (Terman *et al.*, 2002; Humphries *et al.*, 2006) focused on large spiking models that, although contributing much to the discussion, are difficult to analyse mathematically. In addition to these models there are a number of other works not discussed by Nevado Holgado *et al.* (2010) that we shall now discuss, which are highly relevant to our approach.

The inhibitory–excitatory loop architecture of the STN–GP network (sometimes called recurrent inhibition or inhibitory–excitatory network) is common in biology. Wilson & Cowan (1972) have gone so far as to say, ‘all nervous processes of any complexity are dependent upon the interaction of excitatory and inhibitory cells’. This landmark article inspired much research into excitatory–inhibitory populations of neurons. In our article, we have included the signal time delay between neural populations as an extension of the Wilson and Cowan model and find that it can produce oscillations without connections among excitatory neurons (which are necessary for oscillations in the

Wilson and Cowan model). This connection was present in the model by Gillies *et al.* (2002), where their model depended on a strong STN self-interaction term for oscillation onset.

It has been known for some time that network delays are associated with oscillations (Plant, 1981). Combining this idea with the successful Wilson and Cowan model provided new opportunities to study neural populations. Together with the work presented here, another recent article has investigated this extended model (Coombes & Laing, 2009). This work follows the same arguments as our own; however, the analysis remains more general by including two different time delays, one between the neural populations and another for self-interaction terms. The added complication of multiple delays proves more challenging to solve. Biologically, the two delays in our system were similar enough that approximating them with a single delay is appropriate. Indeed, it can be shown that the more general expression of Coombes & Laing (2009) does reduce to the one studied here when the two delay times are equal. Importantly, we show how the single delay equations are solvable with results that closely match simulations of the delay equations. The solution of the two-delay system is left unsolved.

In a recent article closely related to our work, Kumar *et al.* (2011) have shown using a simulation of the STN–GP network that increases in striatal inhibitory input to the GP are enough to cause oscillation onset in their model. Such increase of the striatal input to the GP occurs according to the ‘classical model of Parkinson’s disease’ (Obeso *et al.*, 2000). According to this theory, striatal neurons projecting to the GP express predominantly D2 receptors and are inhibited by dopamine, and thus dopamine loss results in increased inhibition of the GP and subsequent disinhibition of the STN. Several experimental studies confirm the increase in firing rates occurring in the STN, and the decrease seen in GP populations, with the onset of Parkinsonian symptoms (Filion & Tremblay, 1991; Bergman *et al.*, 1994; Raz *et al.*, 2000; Heimer *et al.*, 2002).

As both we and Kumar *et al.* (2011) find that increases in striatal input can cause oscillations in the STN–GP circuit, it is important to compare these findings more closely. Specifically, the model used by Kumar *et al.* (2011) is a leaky integrate-and-fire model composed of 1000 excitatory neurons for the STN population and 2000 inhibitory neurons for the GP population. The connection probability is 5% between the STN and GP population, and 2% among GP neurons. Unlike our model, this model also includes connections among STN neurons with 2% probability. This model uses two different synaptic delay times, 5 ms for connections between the STN and GP and 2 ms for connection among STN and GP neurons. Both populations receive input in the form of uncorrelated Poisson spike trains. Importantly, their model did not explicitly rely on the assumption that the strength of synaptic connections between STN and GP neurons increased due to dopamine loss [which was assumed in previous models by Humphries *et al.* (2006) and Nevado Holgado *et al.* (2010)]. Instead, the simulations showed that increased inhibition from the striatum to GP was sufficient for triggering oscillations in the model.

The level of abstraction of the STN–GP circuit is the most conspicuous difference between Kumar *et al.* (2011) and the firing-rate model that we have presented. Despite this difference, the models share a similar architecture. It is therefore noteworthy that they both show that increasing striatal input can cause oscillation onset. However, whereas the leaky integrate-and-fire model allows simulations of the circuit, our analysis can provide an analytic explanation for why the oscillations occur. We therefore believe that the modelling approaches that lead to these conclusions are complementary and that the results from Kumar *et al.* (2011) are consistent with our conditions for onset of oscillations.

Relationship of model to experimental data

The relationship of the model to experimental data was discussed in detail by Nevado Holgado *et al.* (2010); however, for completeness we shall provide a summary of this discussion.

Our new analysis agrees quantitatively with the old analysis by Nevado Holgado *et al.* (2010) in that the stability conditions given by Eqns 24, 31, 36 and 37 show that a reduction in the synaptic weights w_{SG} and w_{GS} can stop oscillations. This is supported by experimental data. In particular, antiparkinsonian effects have been shown when glutamatergic neurotransmission has been blocked, lending support to the idea that the reduction of w_{SG} can reduce Parkinsonian symptoms (Greenamyre, 1993; Lange *et al.*, 1997). Evidence for w_{GS} comes from a study by Baufreton *et al.* (2005), where it is shown that inhibition from the GP to STN is crucial for beta oscillation generation. They also propose that, in the dopamine-depleted STN, feedback inhibition from the GP is amplified leading to beta oscillations; conversely then, a reduction in w_{GS} may help to alleviate beta oscillations.

It is not obvious, considering the new stability conditions given by Eqns 31 and 37, that reducing the time constant τ will induce beta oscillations; however, it is clear from the more simple conditions given by Eqns 24 and 36. The time constant is influenced by the composition of fast and slow synapses in the population. The time constant can therefore be reduced by increasing the relative numbers of fast and slow synapses. This has been shown to occur (which is equivalent to a decrease in τ) in rodent models of Parkinson’s disease (Shen & Johnson, 2005).

Lastly, the model predicts that cortical input to STN is necessary for the presence of beta oscillations (see Fig. 5). This condition is consistent with the finding of Phillips *et al.* (2006), who showed that blocking metabotropic glutamate receptor 5 receptors in the STN alleviates symptoms in rat models of Parkinson’s disease.

Future work

The benefit of firing-rate models is that they are often mathematically tractable, allowing analytical insights of the system dynamics. However, the limitation of this approach is that it does not include the full range of complex behaviours that can be seen in spiking neural networks. Also, due to the difficulties of solving a system that includes two or more different synaptic transmission delays analytically, our model was restricted to a single variable for this parameter. Therefore, in view of these limitations, a future direction for this work would be to explore a model of this network composed of multiple integrate-and-fire neurons in which the connections between the two populations have heterogeneous delays. The parameters of this stochastic model could be found by deriving the relationship of single neuron parameters to the firing-rate parameters of the model of Nevado Holgado *et al.* (2010). Using this model, we could then check whether the derived stability conditions hold for a spiking neural network.

Another aspect of the model where future research would be useful is elucidation of the relative importance of the separate w_{SG} and w_{GS} connections. As remarked upon in Nevado Holgado *et al.* (2010), there exists some asymmetry in the influence of the weights w_{SG} and w_{GS} . A clearer understanding of this asymmetry would refine our understanding of the process of beta oscillation generation in the STN–GP circuit.

In conclusion, the methods presented are general enough to be of use in analyses of models with similar architectures. It is hoped that, because of the close fit between theory and simulation, these results

will find applications in other assemblies of excitatory and inhibitory neurons, in other brain regions, particularly where time delay signals are significant.

Acknowledgements

This work was supported by EPSRC grant number EP/E501214/1.

Abbreviations

GP, globus pallidus; STN, subthalamic nucleus.

References

- Abbott, L. & Dayan, P. (2001) *Theoretical Neuroscience*. The MIT Press, Cambridge, MA, USA.
- van Albada, S., Gray, R., Drysdale, P. & Robinson, P. (2009) Mean-field modeling of the basal ganglia-thalamocortical system. II Dynamics of parkinsonian oscillations. *J. Theor. Biol.*, **257**, 664–688.
- Asl, F. & Ulsoy, A. (2003) Analysis of a system of linear delay differential equations. *J. Dyn. Syst. Meas. Contr.*, **125**, 215.
- Baufreton, J., Atherton, J., Surmeier, D. & Bevan, M. (2005) Enhancement of excitatory synaptic integration by GABAergic inhibition in the subthalamic nucleus. *J. Neurosci.*, **25**, 8505–8517.
- Bergman, H., Wichmann, T., Karmon, B. & DeLong, M. (1994) The primate subthalamic nucleus. II. Neuronal activity in the MPTP model of parkinsonism. *J. Neurophysiol.*, **72**, 507–520.
- Bevan, M., Magill, P., Terman, D., Bolam, J. & Wilson, C. (2002) Move to the rhythm: oscillations in the subthalamic nucleus-external globus pallidus network. *Trends Neurosci.*, **25**, 525–531.
- Boraud, T., Brown, P., Goldberg, J.A., Graybiel, A.M. & Magill, P.J. (2005) Oscillations in the basal ganglia: the good, the bad, and the unexpected. In Bolam, J., Ingham, C. & Magill, P. (Eds), *The Basal Ganglia VIII*. Springer, New York, pp. 1–24.
- Brown, P. (2003) Oscillatory nature of human basal ganglia activity: relationship to the pathophysiology of Parkinson's disease. *Mov. Disord.*, **18**, 357–363.
- Chen, C.C., Litvak, V., Gilbertson, T., Kuhn, A., Lu, C.-S., Lee, S.-T., Tsai, C.-H., Tisch, S., Limousin, P., Hariz, M. & Brown, P. (2007) Excessive synchronization of basal ganglia neurons at 20 Hz slows movement in Parkinson's disease. *Exp. Neurol.*, **205**, 214–221.
- Coombes, S. & Laing, C. (2009) Delays in activity-based neural networks. *Philos. Transact. A Math. Phys. Eng. Sci.*, **367**, 1117–1129.
- Dorsey, E., Constantinescu, R., Thompson, J., Biglan, K., Holloway, R., Kieburtz, K., Marshall, F., Ravina, B., Schifitto, G., Siderowf, A. & Tanner, C. (2007) Projected number of people with Parkinson disease in the most populous nations, 2005 through 2030. *Neurology*, **68**, 384–386.
- Filion, M. & Tremblay, L. (1991) Abnormal spontaneous activity of globus pallidus neurons in monkeys with MPTP-induced parkinsonism. *Brain Res.*, **547**, 140–144.
- Frank, M., Scheres, A. & Sherman, S. (2007) Understanding decision-making deficits in neurological conditions: insights from models of natural action selection. *Philos. Trans. R. Soc. Lond., B, Biol. Sci.*, **362**, 641–1654.
- Fujimoto, K. & Kita, H. (1993) Response characteristics of subthalamic neurons to the stimulation of the sensorimotor cortex in the rat. *Brain Res.*, **609**, 185–192.
- Gillies, A., Willshaw, D. & Li, Z. (2002) Subthalamic-pallidal interactions are critical in determining normal and abnormal functioning of the basal ganglia. *Proc. Biol. Sci.*, **269**, 545–551.
- Greenamyre, J. (1993) Glutamate-dopamine interactions in the basal ganglia: relationship to Parkinson's disease. *J. Neural Transm.*, **91**, 255–269.
- Hallworth, N.E., Wilson, C.J. & Bevan, M.D. (2003) Apamin-sensitive small conductance calcium-activated potassium channels, through their selective coupling to voltage-gated calcium channels, are critical determinants of the precision, pace, and pattern of action potential generation in rat subthalamic nucleus neurons *in vitro*. *J. Neurosci.*, **23**, 7525–7542.
- Heimer, G., Bar-Gad, I., Goldberg, J. & Bergman, H. (2002) Dopamine replacement therapy reverses abnormal synchronization of pallidal neurons in the 1-methyl-4-phenyl-1,2,3,6-tetrahydropyridine primate model of Parkinsonism. *J. Neurosci.*, **22**, 7850–7855.
- Humphries, M., Stewart, R. & Gurney, K. (2006) A physiologically plausible model of action selection and oscillatory activity in the basal ganglia. *J. Neurosci.*, **26**, 12921–12942.
- Jankovic, J. (2008) Parkinson's disease: clinical features and diagnosis. *J. Neurol. Neurosurg. Psychiatry*, **79**, 368–376.
- Kita, H. (2007) Globus pallidus external segment. *Prog. Brain Res.*, **160**, 111–133.
- Kita, H. & Kitai, S.T. (1991) Intracellular study of rat globus pallidus neurons: membrane properties and responses to neostriatal, subthalamic and nigral stimulation. *Brain Res.*, **564**, 296–305.
- Kita, H., Chang, H.T. & Kitai, S.T. (1983) Pallidal inputs to subthalamus: Intracellular analysis. *Brain Res.*, **264**, 255–265.
- Kita, H., Nambu, A., Kaneda, K., Tachibana, Y. & Takada, M. (2004) Role of ionotropic glutamatergic and GABAergic inputs on the firing activity of neurons in the external pallidum in awake monkeys. *J. Neurophysiol.*, **92**, 3069–3084.
- Kita, H., Tachibana, Y., Nambu, A. & Chiken, S. (2005) Balance of monosynaptic excitatory and disynaptic inhibitory responses of the globus pallidus induced after stimulation of the subthalamic nucleus in the monkey. *J. Neurosci.*, **25**, 8611–8619.
- Kumar, A., Cardanobile, S., Rotter, S. & Aertsen, A. (2011) The role of inhibition in generating and controlling Parkinson's disease oscillations in the basal ganglia. *Front. Syst. Neurosci.*, **5**, 86, doi: 10.3389/fnsys.2011.00086 [online].
- Lang, A. & Zadikoff, C. (2005) Parkinsonian tremor. In Lyons, K. & Pahwa, R. (Eds), *Handbook of Essential Tremor and other Tremor Disorders*. Taylor and Francis, New York, pp. 195–220.
- Lange, K., Kornhuber, J. & Riederer, P. (1997) Dopamine/glutamate interactions in Parkinson's disease. *Neurosci. Biobehav. Rev.*, **21**, 393–400.
- Lau, L. & Breteler, M. (2006) Epidemiology of Parkinson disease. *Neurology*, **5**, 1362–1369.
- Lebedev, M.A. & Wise, S.P. (2000) Oscillations in the premotor cortex: single-unit activity from awake, behaving monkeys. *Exp. Brain Res.*, **130**, 195–215.
- Leblois, A., Boraud, T., Meissner, W., Bergman, H. & Hansel, D. (2006) Competition between feedback loops underlies normal and pathological dynamics in the basal ganglia. *J. Neurosci.*, **26**, 3567–3583.
- Mallet, N., Pogosyan, A., Marton, L.F., Bolam, J.P., Brown, P. & Magill, P.J. (2008a) Parkinsonian beta oscillations in the external globus pallidus and their relationship with subthalamic nucleus activity. *J. Neurosci.*, **28**, 14245–14258.
- Mallet, N., Pogosyan, A., Sharott, A., Csicsvari, J., Bolam, J.P., Brown, P. & Magill, P.J. (2008b) Disrupted dopamine transmission and the emergence of exaggerated beta oscillations in subthalamic nucleus and cerebral cortex. *J. Neurosci.*, **28**, 4795–4806.
- Mazanov, A. & Tognetti, K. (1974) Taylor series expansion of delay differential equations - A warning. *J. Theor. Biol.*, **46**, 271–282.
- Nakanishi, H., Kita, H. & Kitai, S.T. (1987) Intracellular study of rat substantia nigra pars reticulata neurons in an *in vitro* slice preparation: electrical membrane properties and response characteristics to subthalamic stimulation. *Brain Res.*, **437**, 45–55.
- Navado Holgado, A., Terry, J. & Bogacz, R. (2010) Conditions for the generation of beta oscillations in the subthalamic nucleus-globus pallidus network. *J. Neurosci.*, **30**, 12340–12352.
- Obeso, J., Rodriguez-Oroz, M., Rodriguez, M., Lanciego, J., Artieda, J., Gonzalo, N. & Olanow, C. (2000) Pathophysiology of the basal ganglia in Parkinson's disease. *Trends Neurosci.*, **23**, S8–S19.
- Paz, J.T., Deniau, J.-M. & Charpier, S.E. (2005) Rhythmic bursting in the cortico-subthalamo-pallidal network during spontaneous genetically determined spike and wave discharges. *J. Neurosci.*, **25**, 2092–2101.
- Phillips, J., Lam, H., Ackerson, L. & Maidment, N. (2006) Blockade of mGluR₅ glutamate receptors in the subthalamic nucleus ameliorates motor asymmetry in an animal model of Parkinson's disease. *Eur. J. Neurosci.*, **23**, 151–160.
- Plant, R. (1981) A Fitzhugh differential-difference equation modeling recurrent neural feedback. *SIAM J. Appl. Math.*, **40**, 150–162.
- Plenz, D. & Kital, S. (1999) A basal ganglia pacemaker formed by the subthalamic nucleus and external globus pallidus. *Nature*, **400**, 677–682.
- Ray, N., Jenkinson, N., Wang, S., Holland, P., Brittain, J., Joint, C., Stein, J. & Aziz, T. (2008) Local field potential beta activity in the subthalamic nucleus of patients with Parkinson's disease is associated with improvements in bradykinesia after dopamine and deep brain stimulation. *Exp. Neurol.*, **213**, 108–113.

- Raz, A., Vaadia, E. & Bergman, H. (2000) Firing patterns and correlations of spontaneous discharge of pallidal neurons in the normal and the tremulous 1-methyl-4-phenyl-1,2,3,6-tetrahydropyridine vervet model of Parkinsonism. *J. Neurosci.*, **20**, 8559–8571.
- Redgrave, P., Prescott, T.J. & Gurney, K. (1999) The basal ganglia: a vertebrate solution to the selection problem? *Neuroscience*, **89**, 1009–1023.
- Rubin, J. & Terman, D. (2004) High frequency stimulation of the subthalamic nucleus eliminates pathological thalamic rhythmicity in a computational model. *J. Comput. Neurosci.*, **16**, 211–235.
- Schultz, W. & Romo, R. (1988) Neuronal activity in the monkey striatum during the initiation of movements. *Exp. Brain Res.*, **71**, 431–436.
- Shampine, L.F. & Thompson, S. (2001) Solving DDEs in MATLAB. *Appl. Numer. Math.*, **37**, 441–458.
- Shen, K. & Johnson, S. (2005) Dopamine depletion alters responses to glutamate and GABA in the rat subthalamic nucleus. *NeuroReport*, **16**, 171–174.
- Terman, D., Rubin, J., Yew, A. & Wilson, C. (2002) Activity patterns in a model for the subthalamopallidal network of the basal ganglia. *J. Neurosci.*, **22**, 2963–2976.
- Vogels, T., Rajan, K. & Abbott, L. (2005) Neural network dynamics. *Annu. Rev. Neurosci.*, **28**, 357–376.
- Wilson, H. & Cowan, J. (1972) Excitatory and inhibitory interactions in localized populations of model neurons. *Biophys. J.*, **12**, 1–24.